Quantum Hall Ferromagnetism in the Presence of Tunable Disorder

W. Pan, J. L. Reno, D. Li, and S. R. J. Brueck

Phys. Rev. Lett. **106**, 156806 — Published 13 April 2011

DOI: 10.1103/PhysRevLett.106.156806

Quantum Hall Ferromagnetism in the Presence of Tunable Disorder

W. Pan[1], J.L. Reno[1], D. Li[2], and S.R.J. Brueck[2]

[1] Sandia National Laboratories, P.O. Box 5800, Albuquerque, NM 87185

[2] Center for High Technology Materials, University of New Mexico, Albuquerque, NM 87108

In this Letter, we report our recent experimental results on the energy gap of the ν=1 quantum Hall state ($\Delta_{\nu=1}$) in a quantum antidot array sample, where the "effective" disorder potential can be tuned continuously. $\Delta_{\nu=1}$ is nearly constant at small effective disorders, and collapses at a critical disorder. Moreover, in the weak disorder regime, $\Delta_{\nu=1}$ shows a $B_{total}^{1/2}$ dependence in tilted magnetic field measurements, while in the strong disorder regime, $\Delta_{\nu=1}$ is linear in B_{total}; where B_{total} is the total magnetic field at ν=1. We discuss our results within several models involving the quantum Hall ferromagnetic ground state and its interplay with sample disorder.

PACS numbers: 73.43.-f, 71.10.-w, 73.23.-b

Electron-electron (e-e) interaction plays an important role in two-dimensional electron systems (2DES) and is known to induce unexpected many-body ground states. One notable example is the fractional quantum Hall effect (FQHE) [1-3]. In this regime, due to a strong e-e interaction in the presence of quantizing magnetic fields, the 2DES forms a new type of incompressible liquid whose low energy excitations bear fractional charges [2,4,5]. In contrast, the physics of the integer quantum Hall effect (IQHE) [6] can be understood in a single particle picture of Landau level quantization and disorder broadening [7]. However, many-particle effects can contribute to the magnitude of the IQHE, such as in the case of the ν=1 state, where ν is the Landau level filling factor. In a single particle picture, the energy gap at this filling is due to the Zeeman splitting and equal to $|g|\mu_B B$, where g = - 0.44 is the effective Landé g-factor in GaAs, μ_B is the Bohr magneton, and B is the magnetic field. Experimentally, the measured value is much larger than this single particle splitting. This is the result of strong Coulombic e-e interaction [8,9], which forces electron spins to align at ν=1 with the applied magnetic field. The ground state displays many-body quantum Hall ferromagnetism (QHF) [10], which gives rise to a large energy gap. Away from ν=1, a small change in ν has been shown to lead to significant depolarization and Skyrmions are formed [11,12].

Aside from e-e interactions, disorder has a similarly important impact on energy gaps in 2DES and their interplay remains a major line of research. In fact, the much debated apparent two-dimensional metal-to-insulator transition at zero B field in high quality, yet disordered 2DES's is considered to arise from this interplay [13]. Moreover, it has been shown that the competition between disorder and e-e interactions can induce a collapse of the spin splitting at low B fields and large ν's [14]. In the case of the ν=1 QHF ground state, many theoretical studies [15-18] have been devoted to understand how disorder

would affect the ferromagnetic order. In one series of studies, it was shown that with increasing disorder, eventually, the ferromagnetic state would be destroyed and the ground state undergo a quantum phase transition to, for example, a paramagnetic [15] or a QH spin glass (QHSG) state [18].

To date, almost all electronic transport studies on the $\nu=1$ state have been carried out in the clean limit [19-22], where the QHF ground state prevails. Little has been done in examining the possible phase transition from QHF to other ground states as a function of increasing disorder. This lack of data mainly originates from the difficulty of realizing an in-situ tunable disorder.

In this letter, we study the $\nu=1$ state in a 2D quantum antidot array sample. By controlling the ratio of the electronic potential modulation strength to the 2DES Fermi energy, i.e., the "effective disorder" (ED), we have observed a sudden collapse of the $\nu=1$ energy gap ($\Delta_{\nu=1}$) at an apparent critical disorder, indicating a possible transition from a QHF to a QHSG. At small effective disorders $\Delta_{\nu=1}$ is nearly constant. Around ED ~ 0.08, $\Delta_{\nu=1}$ drops sharply from ~ 11K at ED = 0.0786 to ~ 1.6 K at ED = 0.0804. Furthermore, in tilted magnetic field measurements $\Delta_{\nu=1}$ shows a $B_{total}^{1/2}$ dependence at ED =0.0786, indicating that the QHF ground state prevails, whereas at ED =0.0804 $\Delta_{\nu=1}$ is linear with B_{total}, suggesting a QHSG state. In the following we focus on data from one specimen, although a second sample from a different wafer showed the identical behavior.

The starting material is a high mobility 2DES realized in a GaAs quantum well (QW) heterostructure. The QW is 200 nm below the sample surface and the well width is 30 nm. The as-grown 2DES has an electron density of 1.9×10^{11} cm^{-2} and a mobility of 3×10^{6} cm^2/Vs. The antidot array is fabricated using state-of-the-art interferometric lithography [23] and chemical wet etching. The finished antidot array has a pitch of ~ 350 nm and antidot diameter of ~ 150 nm. An SEM picture of a fabricated sample is shown in the inset of Figure 1. The 2DES density in the patterned sample can be tuned , in-situ, from ~ 0.3×10^{11} to 2.3×10^{11} cm^{-2} by a low temperature red light-emitting diode (LED) illumination.

In Fig.1a, we show the diagonal resistance R_{xx} and Hall resistance R_{xy} traces for this sample over a wide range of B. Well developed IQHE states are observed at ν=1, 2, 3,… Fig. 1b focuses on the R_{xx} data around B = 0. Several features are worth emphasizing. First, there is a positive magnetoresistance (MR) around B = 0 and a local maximum at B ~ 0.1T. They have been observed in previous experiments on quantum antidot array samples, and can be attributed to magnetic breakdown in the presence of modulation [24]. Using the value of the magnetic field (B_p) at the local R_{xx} maximum and following the standard analysis [24,25], we estimate a potential modulation strength of ΔV ~ 1.5 meV in our antidot array sample. Second, commensurability oscillations (CO) [26] occur at low magnetic fields, marked by the upward triangles. From their period in 1/B (Fig.1c) an antidot periodicity of ~ 380 nm is deduced, which is consistent with the design value of 350 nm. Third, Shubnikov de-Haas (SdH) oscillations occur at higher B field, marked by the downward triangles, from which the 2DES density is determined.

Figure 2a shows the temperature (T) dependence of R_{xx} in high B fields. Over the whole temperature range, the ν=2 QH state remains strong and its resistance minimum vanishingly small. On the other hand, the ν=1 state shows a very strong temperature dependence, with R_{xx} rising from a vanishingly small value at T = 1.2 K to R_{xx} ~ 2700 Ω at 2.3K Figure 2b shows the activation plot for the R_{xx} minimum at ν=1 and an energy gap of ~ 19 K is deduced from the linear fit to the data points.

We have carried out a systematic density dependent study of the ν=1 energy gap. The electron density was continuously tuned by applying different doses of LED illumination. Figure 3a shows the energy gap as a function of the effective disorder (ED). The effective disorder is quantified as ED = B_p/n, where B_p is the magnetic field of the local maximum around B = 0, which is proportional to ΔV, the antidot potential modulation strength. n is the 2DES density and proportional to E_F, the 2DES Fermi energy. In a sample without antidot array (ED=0), $\Delta_{\nu=1}$ exceeds the Zeeman energy, by at least a factor of ~ 10, due to the formation of a ferromagnetic ground state. As ED increases into the weak effective disorder regime, $\Delta_{\nu=1}$ decreases only slowly (e.g. from ~ 24 K at ED=0 to ~ 23K at ED ~ 0.04). The decrease accelerates as ED continues to increase until $\Delta_{\nu=1}$ drops sharply over a narrow range from ~11 K at ED = 0.0786 to ~ 1.6K at ED = 0.0804.

Figure 4 shows the tilted B field dependence at two effective disorders. Here $\Delta_{\nu=1}$ is plotted against the total magnetic field B_{total} = B/cos(θ), the actual magnetic field at which ν=1 occurs at tilt angle θ. At ED = 0.0786, $\Delta_{\nu=1}$ is better fitted by a $B_{total}^{1/2}$ dependence,

characteristic of the ν=1 QHF state [19]. At ED =0.0804, $\Delta_{\nu=1}$ is clearly linear in B_{total}, with a slope of ~3|g|μ_B (g=-0.44 in GaAs).

The collapse of $\Delta_{\nu=1}$ at a critical disorder is surprising. Before discussing the possible physical origin of this collapse, we want to convey that indeed B_p/n ($\propto \Delta V/E_F$) is a good measure for effective disorder in our antidot array sample. The introduction of antidots creates, in the energy vs. position plot in Figure 3b, a modulated bottom of the energy band by a strength of ΔV. This modulation can be viewed as voids, or large scattering centers for electron transport. When the 2DES density is high, for example n = $2x10^{11}$ cm^{-2} then E_F ~ 7 meV which is much larger than ΔV (~1.5 meV). Consequently, the electrons at the Fermi level experience little influence from the antidots. On the other hand, at smaller 2DES densities, for example n=$3x10^{10}$ cm^{-2}, E_F ~ 1 meV, which is of the same order as ΔV. In this case, electrons at the Fermi level are strongly influenced by the presence of antidots, and the effective disorder strength is large.

We shall note here that the disorder dependence of $\Delta_{\nu=1}$ in Fig.3a resembles that of the collapse of the spin splitting theoretically predicted in Ref. [14] and experimentally examined in Ref. [27]. It is not known whether the same mechanism is also responsible for our observation at ν=1 in *high* magnetic fields, since only high Landau level fillings ($\nu \geq 2$, or *low* magnetic fields) were considered in Ref. [14] for this transition.

As for other possible mechanisms for the collapse of $\Delta_{\nu=1}$, the most direct explanation is that increased disorder reduces the 2DES mobility, which increases Landau level broadening and, in turn, closes the gap. In this case, we expect a smooth reduction in energy gap [28] and no sharp change in the ν=1 gap should be expected at any “critical”

disorder value. Furthermore, the charge excitation gap at $\nu=2$ is only weakly influenced by the presence of the anti-dot array. As shown in Fig. 2(a), the resistance minimum at $\nu=2$ remaining vanishingly small at ~ 2.3K, while at $\nu=1$ the minimum has risen to ~2700 Ω.

Another possible mechanism is density inhomogeneity. With the introduction of antidots, the 2DES density becomes non-uniform, especially around the edges of antidots. Thus, when the 2DES is globally in a QH state at a particular ν (e.g. $\nu=1$) there are regions where ν is either larger or smaller than 1 [29] and the $\nu=1$ QH state only exists in narrow stripes [30]. As the temperature is raised, in this non-uniform system, the quasi-electrons are readily becoming delocalized and the energy gap of the state is reduced. Again, this model should apply for both the $\nu=2$ and $\nu=1$ QH states, in contrast to our data. Furthermore, in this model, the effective disorder dependence of $\Delta_{\nu=1}$ should be gradual and not abrupt, as seen in Figure 3.

Considering density inhomogeneity, we address here two possible mechanisms that can lead to a reduction in energy gap, i.e., the formation of edge spin textures [31] and quick depolarization away from $\nu=1$ [11]. Within the edge spin textures model, it has been shown that a soft edge [32], such as the one created by the chemical etching in our antidot sample, can reduce the energy gap at $\nu=1$. It is unlikely that the formation of spin textures at soft edges can explain our data, since this model does not imply a sudden collapse of the gap. As for the second mechanism, in Ref. [11] it was observed that the 2D system was fully polarized only at $\nu=1$. A small change in ν leads to significant depolarization. Applying this observation to our experiment, we note that, as the electron

density decreases and ED increases, the percentage area in which the electron density is different from the global average density increases. Consequently, there are more regions where ν is not exactly at 1. The depolarization effect then can lead to a reduction in the ν=1 activation energy at large ED. However, a basic modeling taking into account the linear decrease in polarization around ν=1 [11] and a simple density inhomogeniety profile [31] cannot explain the sudden collapse of $\Delta_{\nu=1}$ as ED increases from 0.0796 to 0.0804.

Finally, in a series of papers it has been shown that disorder can play an important role in establishing the nature of the ground state at ν=1 in the QH regime [15-18]. In the weak disorder regime, the ground state is a ferromagnetic state [10] and $\Delta_{\nu=1}$ is dominated by e-e interactions and, thus, large. As the amount of disorder increases, the ground state transitions into a paramagnetic state [15], or QHSG state [18] where single spin flips dominate the energy gap at ν=1. The disorder dependence of our data on the ν=1 energy gap is consistent with this picture. The rapid drop of $\Delta_{\nu=1}$ at an apparently critical disorder value suggests that the transition may be of first order, consistent with the theoretical prediction of the QHSG transition [18]. Furthermore, in the QHSG regime $\Delta_{\nu=1}$ is expected to show a linear B_{total} dependence as the Zeeman splitting now dominates the energy gap. Indeed, as shown in Fig.4b, $\Delta_{\nu=1}$ at ED~ 0.08 is linear with B_{total}. The deduced energy gap is indeed small and on the order of $|g|\mu_B B$, although it exceeds this value by a factor of 3. The origin for this discrepancy is unclear but may be related to the formation of spin clusters in the QHSG regime.

In summary, we have measured the energy gap at $\nu=1$ as a function of effective disorder potential in a 2D quantum antidot array sample. The energy gap is nearly constant at small effective disorder and collapses at a critical disorder. Most theoretical models for this regime cannot account for the sum of our findings, except for a model that implies a quantum phase transition from a quantum Hall ferromagnetic ground state to a quantum Hall spin glass state as disorder increases.

We thank Denise Tibbetts and Mike Smith for their excellent technical assistance, and J.A. Simmons, J.K. Jain, H.A. Fertig, M. Berciu, and C. Zhou for helpful discussions. This work was supported by the DOE Office of Basic Energy Sciences. Sandia National Laboratories is a multi-program laboratory managed and operated by Sandia Corporation, a wholly owned subsidiary of Lockheed Martin company, for the U.S. Department of Energy's National Nuclear Security Administration under contract DE-AC04-94AL85000. The facilities of the NSF-sponsored NNIN node at the University of New Mexico were used for the antidot array fabrication.

Reference:

1. D.C. Tsui, H.L. Stormer, and A.C. Gossard, Phys. Rev. Lett. **48**, 1559 (1982).
2. R.B. Laughlin, Phys. Rev. Lett. **50**, 1395 (1983).
3. J.K. Jain, Phys. Rev. Lett. **63**, 199 (1989)
4. R. De-Picciotto *et al.*, Nature **389**, 162 (1997).
5. L. Saminadayar *et al.*, Phys. Rev. Lett. **45**, 494 (1980).
7. *The Quantum Hall Effect*, edited by R.E. Prange and S.M. Girvin (Springer-Verlag, New York, 1987).
8. S. Sondhi *et al.*, Phys. Rev. B **47**, 16419 (1993).
9. H.A. Fertig *et al.*, Phys. Rev. B **50**, 11018 (1994).
10. See, for example, the review article by S.M. Girvin and A.H. Macdonald in *Perspectives in Quantum Hall Effects*, edited by S. Das Sarma and A. Pinczuk (Wiley Interscience, New York, 1997).
11. P. Plochocka *et al.*, Phys. Rev.Lett. **102**, 126806 (2009).
12. S.E. Barrett *et al.*, Phys. Rev. Lett. **74**, 5112 (1995).
13. B. Spivak *et al.*, Rev. Mod. Phys. **82**, 1743 (2010).
14 M.M. Fogler and B.I. Shklovskii, Phys. Rev. B **52**, 17366 (1995).
15. J. Sinova, A.H. MacDonald, and S.M. Girvin, Phys. Rev. B **62**, 13579 (2000).
16. G. Murthy, Phys. Rev. B **64**, 241309 (2001).
17. S. Dickmann, Phys. Rev. B **65**, 195310 (2002).
18. S. Rapsch, J. T. Chalker, and D. K. K. Lee, Phys. Rev. Lett. **88**, 036801 (2002).
19. A. Schmeller *et al.*, Phys. Rev. Lett. **75**, 4290 (1995).
20. D.K. Maude *et al.*, Phys. Rev. Lett.**77**, 4604 (1996).
21. D.R. Leadley *et al.*, Semicon. Sci. Technol. **13**, 671 (1998).
22. S.P. Shukla *et al.*, Phys. Rev. B **61**, 4469 (2000).
23. S. C. Lee and S. R. J. Brueck, J. Vac. Sci. Technol. B **22**, 1949 (2004).
24. P. H. Benton *et al.*, Phys. Rev. B **42**, 9229 (1990).
25. C. Albrecht *et al.*, Phys. Rev. Lett. **83**, 2234 (1999).
26. D. Weiss *et al.*, Phys. Rev. Lett. **66**, 2790 (1991).
27. B.A. Piot *et al.*, Phys. Rev. B **75**, 155332 (2007).
28. D.N. Sheng *et al.*, Phys. Rev. Lett. **90**, 256802 (2003).
29. D.B. Chklovskii, B.I. Shklovskii, and L.I. Glazman, Phys. Rev. B **46**, 4026 (1992).
30. A.L. Efros, Phys. Rev. B **45**, 11354 (1992).
31. J. Sjöstrand, A. Eklund, A. Karlhede, Phys. Rev. B **66**, 165308 (2002).
32. M. Kato *et al.*, Phys. Rev. Lett. **102**, 086802 (2009).

Figure captions:

Figure 1: (a) R_{xx} and R_{xy} in a quantum antidot array sample. The IQHE states at ν =1,2,3 are marked. The inset shows an SEM picture of the device. (b) R_{xx} around B = 0. The arrows mark the B field positions where R_{xx} reaches a local maximum. The downward triangles mark the Shubnikov de Haas (SdH) oscillations, and the upward triangles the commensurate oscillations (CO). (c) Fan diagram for the SdH oscillations and CO. From the slope of their linear fits, the electron density and the period of the electronic potential modulation can be deduced. N denotes the Landau level filling factor in the case of the SdH oscillations and an integer value assigned to the R_{xx} minimum in the case of the CO.

Figure 2: (a) Temperature dependence of R_{xx}. (b) Activation plot for the R_{xx} minimum at ν=1. The line is a linear fit to the data points.

Figure 3: (a) The ν=1 energy gap as a function of effective disorder, defined as B_p/n. (b) Illustration of the strength of the effective disorder in a quantum antidot device.

Figure 4: Tilt magnetic field dependence of the ν=1 energy gap at ED=0.0786 (upper panel) and ED=0.0804 (bottom panel). The line in the upper panel shows a $B_{total}^{1/2}$ dependence and the line in the bottom panel is a linear fit.

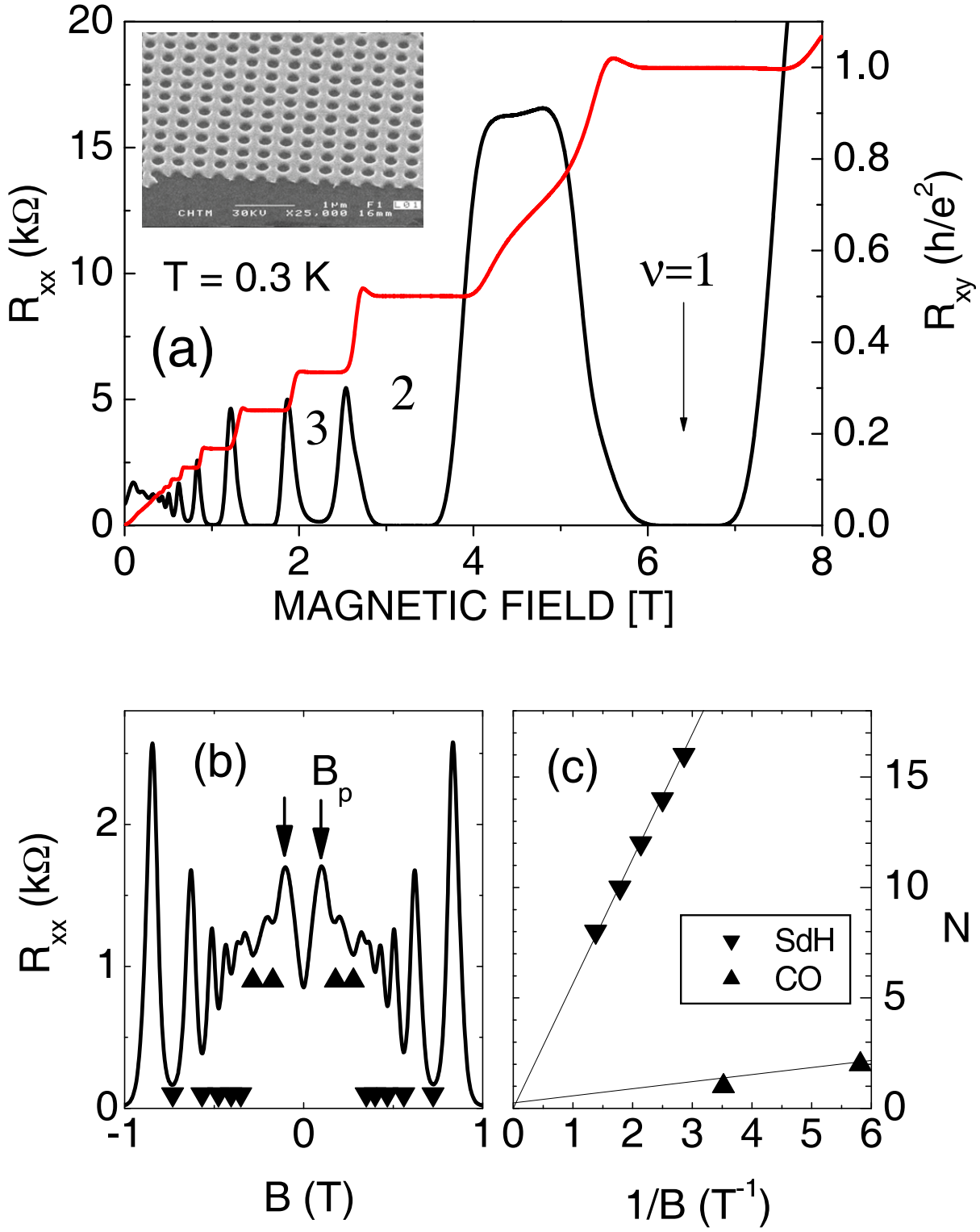

Figure 1 LW12031 10MAR2011

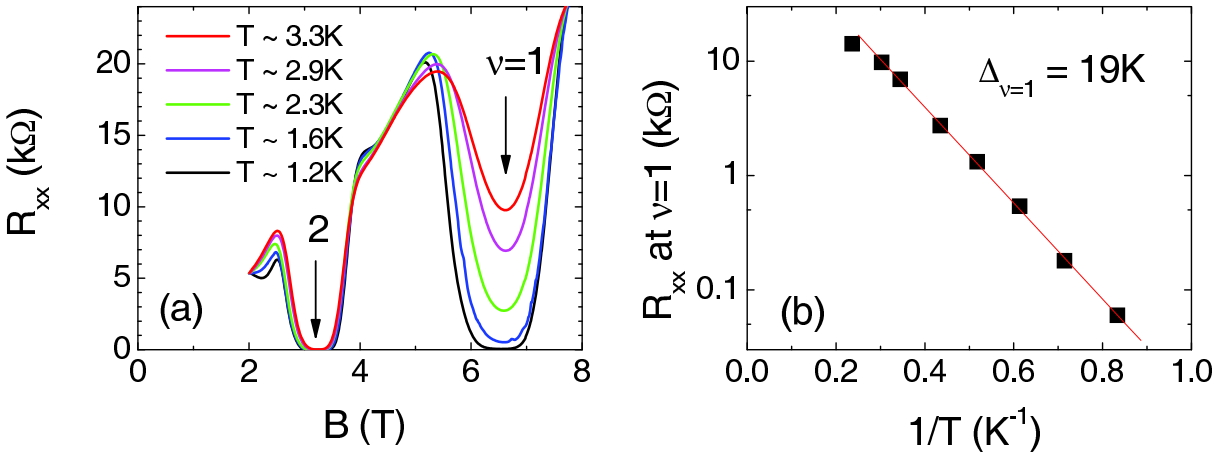

Figure 2 LW12031 10MAR2011

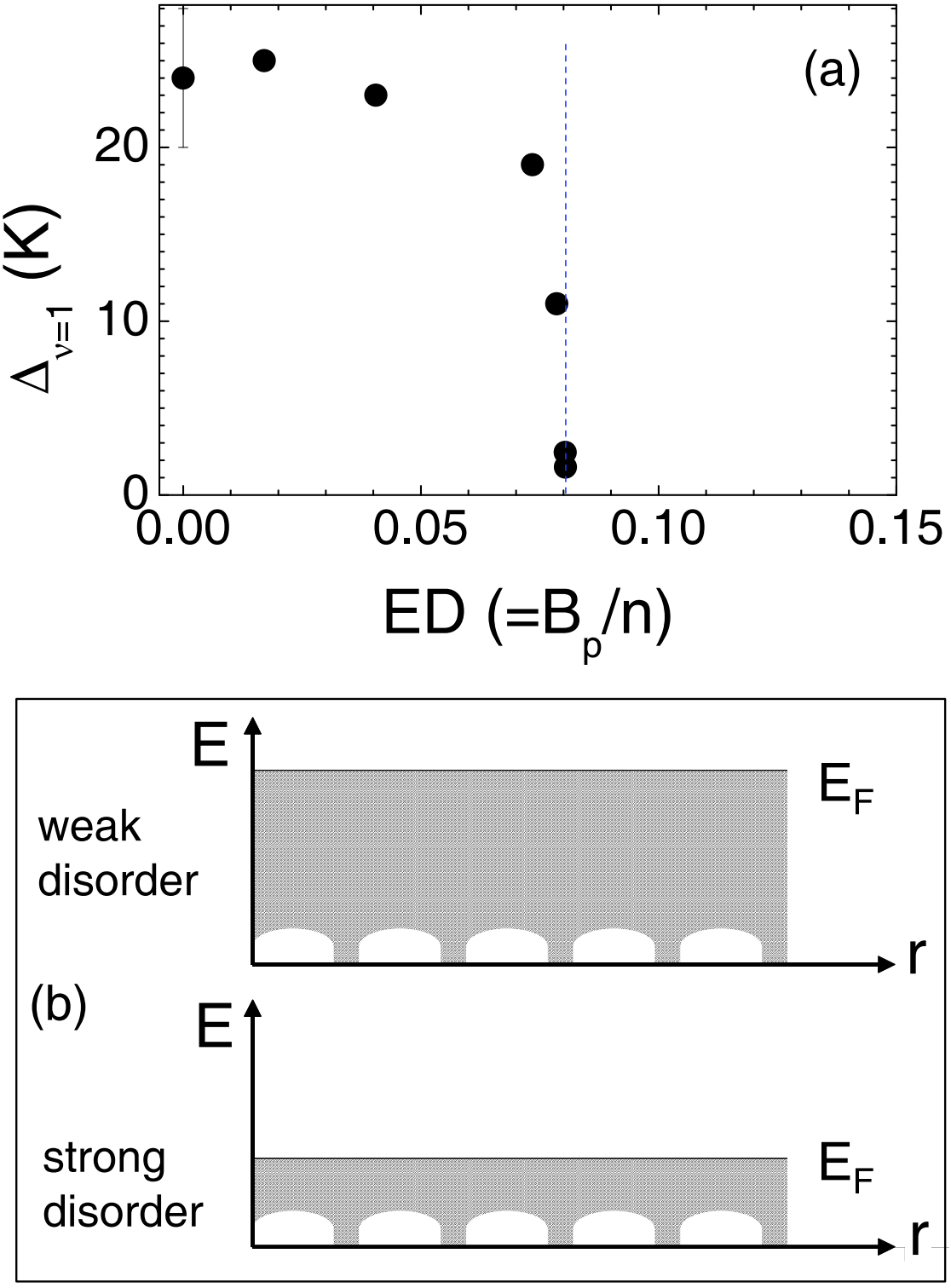

Figure 3 LW12031 10MAR2011

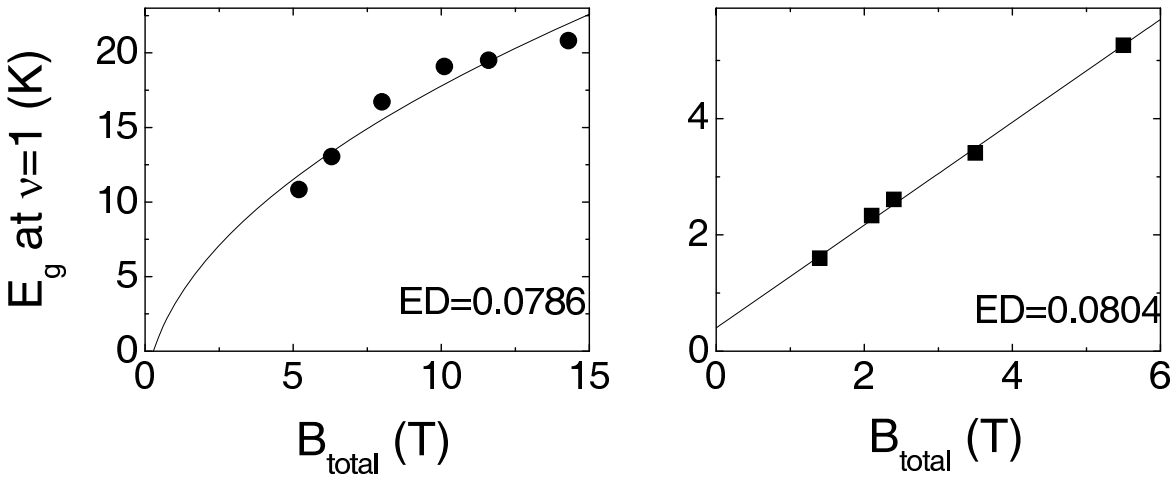

Figure 4 LW12031 10MAR2011